Dyes and Pigments 86 (2010) 259–265

Contents lists available at ScienceDirect

Dyes and Pigments

journal homepage: www.elsevier.com/locate/dyepig

Development of liquid crystal embedded in polymer electrolytes composed of click polymers for dye-sensitized solar cell applications

Md. Anwarul Karim [a,d], Myungkwan Song [a], Jin Su Park [a], Yeol Ho Kim [a], Myung Jin Lee [a], Jae Wook Lee [b,*], Chan Woo Lee [c], Young-Rae Cho [d], Yeong-Soon Gal [e], Jun Hee Lee [f], Sung-Ho Jin [a,*]

[a] Department of Chemistry Education, Interdisciplinary Program of Advanced Information and Display Materials, and Center for Plastic Information System, Pusan National University, Busan 609-735, Korea
[b] Department of Chemistry, Dong-A University, Busan 604-714, Korea
[c] Department of Chemistry, University of Ulsan, Ulsan 680-749, Korea
[d] Department of Materials Science and Engineering, Pusan National University, Busan 609-735, Korea
[e] Polymer Chemistry Laboratory, Kyungil University, Hayang 712-701, Korea
[f] Department of Advanced Materials Engineering, Dong-A University, Busan 604-714, Korea

ARTICLE INFO

Article history:
Received 17 October 2009
Received in revised form
22 January 2010
Accepted 24 January 2010
Available online 1 February 2010

Keywords:
Catalyzed click polymer
Non-catalyzed click polymer
Polymer electrolyte
Liquid crystal
Dye-sensitized solar cell
Photovoltaic performance

ABSTRACT

Two different methods were used to synthesize fluorene-based click polymers, and their effects on their photovoltaic performance in dye-sensitized solar cells were compared. The dye-sensitized solar cells with a configuration of SnO_2:F/TiO_2/N719 dye/polymer electrolyte/Pt devices were fabricated using these click polymers as the electrolyte components. We also compared the photovoltaic performance of these liquid crystal embedded in click polymers to that of poly(acrylonitrile). Among the devices, the device composed of the Cu^I-catalyzed click polymer exhibited high power conversion efficiency of 4.70% at 1 sun, which was as high as that of the poly(acrylonitrile)-composed polymer electrolyte.

1. Introduction

Highly efficient dye-sensitized solar cells (DSSCs) based on nanocrystalline TiO_2 (nc-TiO_2) and photoexcited dye molecules have attracted much attention as potential alternatives to traditional photovoltaic devices [1–3]. The overall power conversion efficiency (PCE) of DSSCs based on liquid electrolytes reached 11% under irradiation of 100 mW cm^{-2} (AM 1.5) [4,5]. Growing attention has been paid to DSSCs using polymer and/or gel electrolytes, owing to their unique hybrid network structure and favourable characteristics such as negligible vapour pressure and good filling properties with the nc-TiO_2 electrode and counter electrode, as well as high ionic conductivity, which is achieved by trapping liquid electrolyte in polymer cages formed in a host matrix [6,7]. Hence, polymer and/or gel electrolytes have attracted considerable interest for diverse applications.

Although, in the reaction of click chemistry, Cu^I-catalyzed 1,3-dipolar cycloaddition is a favourable reaction, it suffers the drawbacks of long reaction time, poor product solubility, [8] and difficult removal of the metal from the resulting polymer. Catalyst residues can be detrimental to both the electronic and optical properties of polymers as light emissions from π-conjugated polymers can be quenched by metallic traps [9].

To extend previous work [10], this paper concerns the synthesis and characterization of click polymers obtained from 2,7-diazido-9,9-dioctylfluorene and 2,7-diethynyl-9,9-dioctylfluorene using Cu^I-catalyzed and non-Cu^I-catalyzed click polymerization. These polymers were employed as a polymer matrix to trap the liquid electrolyte and form the polymer electrolyte. The photovoltaic performance of the polymers in DSSCs with a device configuration of SnO_2:F/TiO_2/N719 dye/polymer electrolyte/Pt were compared with those of a poly(acrylonitrile) (PAN)-based polymer electrolyte. A liquid crystal was also used as a component of a polymer electrolyte for the fabrication of DSSCs in order to improve photovoltaic performance as previously reported [11].

This study focuses on the synthesis of soluble, click polymers using Cu^I- and non-Cu^I-catalyzed click reaction methods and compares the electro-optical properties of the polymers and the

* Corresponding authors. Tel.: +82 51 510 2727; fax: +82 51 581 2348.
E-mail addresses: jlee@donga.ac.kr (J.W. Lee), shjin@pusan.ac.kr (S.-H. Jin).

0143-7208/$ – see front matter © 2010 Elsevier Ltd. All rights reserved.
doi:10.1016/j.dyepig.2010.01.012

photovoltaic performances of DSSCs with respect to poly(acrylonitrile) (PAN)-based polymer electrolyte.

2. Experimental

2.1. Materials and characterization

2,7-Diazido-9,9-dioctylfluorene [12] and 2,7-diethynyl-9,9-dioctylfluorene [13,14] were synthesized using a slight modification of the method reported in the literature. All reagents were purchased from Sigma–Aldrich Co., and used without further purification. The solvents were purified using normal procedures and were handled in a moisture-free atmosphere. Column chromatography was carried out using silica gel (Merck, 250–430 mesh). Conventional Schlenk techniques were used and the reactions were carried out under a N_2 atmosphere unless otherwise noted. The ^{1}H-NMR spectra were recorded on a Bruker AM-300 spectrometer and the chemical shifts were recorded in ppm units with chloroform as an internal standard. The absorption and photoluminescence (PL) spectra were measured by using a Shimadzu UV-3100 UV-visible spectrometer and a Hitachi F-4500 fluorescence spectrophotometer, respectively. The solid-state emission measurements were carried out by supporting each film on a quartz substrate that was mounted to receive front-face excitation at an angle 45°. Each polymer film was excited with several portions of the visible spectrum from a xenon lamp. The molecular weight and polydispersity of the polymer were determined by gel permeation chromatography (GPC) using a Plgel 5 μm MIXED-C column on an Agilent 1100 series liquid chromatography system with tetrahydrofuran (THF) as an eluent and polystyrene standards being used for calibration. Thermal analyses were carried out on a Mettler Toledo TGA/SDTA 851, DSC 822 analyzer under an N_2 atmosphere at a heating rate of 10 °C min^{-1}. Cyclic voltammetry (CV) was carried out using a Bioanalytical Systems CV-50 W voltammetric analyzer at a potential scan rate of 50–100 mV s^{-1} in a 0.1 M solution of tetrabutylammonium tetrafluoroborate (Bu_4NBF_4) in anhydrous acetonitrile. Each polymer film was coated on a platinum (Pt) disc electrode (0.2 cm^2) by dipping the electrode into a solution of the polymer (10 mg mL^{-1}). A Pt wire and an $Ag/AgNO_3$ electrode were used as the counter and reference electrodes, respectively. All the electrochemical experiments were carried out in a glove box under an Ar atmosphere at room temperature.

2.2. Cu^I-catalyzed click reaction method for the synthesis of polymer, P1

In a flame dried Schlenk flask, 2,7-diazido-9,9-dioctylfluorene and 2,7-diethynyl-9,9-dioctylfluorene monomers (1:1 equiv.) and sodium L-ascorbate (10 mol%) were dissolved in THF (2–3 mL) under a N_2 atmosphere and triethylamine (TEA) (0.2–0.3 mL) was added as a ligand [10,15]. The flask was flushed with N_2 for 20–30 min and the mixture was frozen and evacuated three times and $CuSO_4 \cdot 5H_2O$ (5 mol%) was added under N_2 gas. The mixture was stirred at 30–35 °C for 48 h. After completion of the click polymerization, THF was removed under vacuum and the mixture was dissolved in chloroform, washed with aqueous NH_4OH solution followed by water. The organic layer was separated and the solvent was removed. The resulting polymer was precipitated in methanol. In the above procedure, the reaction will not proceed if TEA is not added, even after 10 days at room temperature. By adding TEA and increasing the reaction temperature, we were able to synthesize the desired polymer. A recent systematic investigation conducted in organic media revealed that aliphatic amine ligands consistently led to significantly faster rates compared to other amines. This could be due to a number of factors, including electron back donation from the copper center to the alkyne, and the stronger basicity and enhanced ability of aliphatic amine ligands relative to pyridine-based ligands [16].

2.2.1. Polymer P1 (yield: 92%)

Yellow solid. ^{1}H-NMR ($CDCl_3$, 500 MHz): δ (ppm) 8.39 (s), 8.35 (s), 8.03 (s), 7.95–7.91 (m), 7.86–7.79 (m), 7.78–7.73 (m), 7.09–7.07 (m), 7.03 (d), 2.19–2.10 (m), 2.05–1.99 (m), 1.27–1.10 (m), 0.95–0.78 (m), 0.72–0.66 (m). Anal Calcd for $(C_{62}H_{82}N_6)_n$: C, 81.71; H, 9.06, N, 9.22. Found: C, 80.18: H, 9.29; N, 9.26.

2.3. Non-Cu^I-catalyzed click reaction method for the synthesis of polymer, P2

Diazide- and diethynyl-based monomers (1:1 equiv.) were placed in a flame dried Schlenk flask and a mixture of DMF/toluene (1:1, volume ratio) was injected. The reaction mixture was stirred under N_2 gas at 100 °C for 24 h after which time, the reaction mixture was diluted with chloroform and a mixture of hexane and chloroform (10:1) were added dropwise through a cotton filter with stirring. The precipitates were allowed to stand overnight, collected by filtration, and dried under vacuum at room temperature [9].

2.3.1. Polymer P2 (yield: 91%)

Yellow solid. ^{1}H-NMR ($CDCl_3$, 300 MHz): δ (ppm) 8.35 (s), 7.98–7.94 (m), 7.89–7.84 (m), 7.76–7.74 (m), 7.66–7.58 (m), 7.48–7.43 (m), 7.32 (s), 7.02 (s), 2.18 (m), 2.01–1.82 (m), 1.25–1.08 (m), 0.81 (m), 0.66 (m). Anal Calcd for $(C_{62}H_{82}N_6)_n$: C, 81.71; H, 9.06, N, 9.22. Found: C, 80.35: H, 9.41; N, 9.30.

2.4. Fabrication of DSSCs

DSSCs were fabricated as follows. Screen-printable nc-TiO_2 pastes were prepared using ethyl cellulose (Aldrich), lauric acid (Fluka) and terpineol (Fluka) as described elsewhere [17]. The prepared nc-TiO_2 paste was coated on a FTO conducting glass (TEC8, Pilkington, 8 Ω cm^{-1}, glass thickness of 2.3 mm), dried in air at an ambient temperature for 5 min and sintered at 500 °C for 30 min. The thicknesses of the annealed films were measured with Alpha-step IQ surface profiler (KLA Tencor). For dye adsorption, the annealed nc-TiO_2 electrodes were immersed in absolute ethanol containing 0.5 mM of N719 dye ($Ru[LL'(NCS)_2]$, L = 2,2′-bypyridyl-4,4′-dicarboxylic acid, L′ = 2,2′-bypyridyl-4,4′-ditetrabutylammonium carboxylate) for 24 h at an ambient temperature. Pt counter electrodes were prepared by thermal reduction of thin film formed from 7 mM of H_2PtCl_6 in 2-propanol solution at 400 °C for 20 min. The dye-adsorbed nc-TiO_2 electrode and Pt counter electrode were assembled using 60 μm thick Surlyn (Dupont 1702). The polymer electrolyte was composed of I_2, tetrabutylammonium iodide (TBAI), 1-propyl-3-methylimidazolium iodide (PMII), ethylene carbonate/propylene carbonate (EC/PC, 3/1 as weight ratio), PAN (M_w = 86,200, Aldrich Co) or click polymers as a polymer matrix, liquid crystal (ML-0249) (Merck Co) as a plasticizer, and acetonitrile. The ML-0249 is currently used for thin film transistor liquid crystal displays due to its advantages of fast response time and low driving voltage. The polymer electrolytes were filled between two electrodes using a vacuum pump in hotplate. A uniform polymer electrolyte layer was formed in the DSSCs after cooling down to room temperature. The active areas of dye-coated TiO_2 films were measured by an image analysis program equipped with a digital microscope camera (Moticam 1000). The performance of DSSCs were measured using a calibrated AM 1.5G solar simulator (Orel 300 W simulator, models 81150) with a light intensity of 100 mW cm^{-2} adjusted using a standard PV reference cell (2 × 2 cm monocrystalline silicon solar cell, calibrated at NREL, CO, USA) and a computer-controlled Keithley 236 source measure unit.

The PCE (η) of a solar cell given by

$$\eta = P_{out}/P_{in} = (J_{sc} \times V_{oc}) \times FF/P_{in}$$

with $FF = P_{max}/(J_{sc} \times V_{oc}) = (J_{max} \times V_{max})/(J_{sc} \times V_{oc})$, where P_{out} is the output electrical power of the device under illumination, and P_{in} is the intensity of incident light (e.g. in Wm^{-2} or $mW\ cm^{-2}$). V_{oc} is the open-circuit voltage, J_{sc} is the short-circuit current density, and fill factor (FF) is calculated from the values of V_{oc}, J_{sc}, and the maximum power point, P_{max}. All fabrication steps and characterization measurements were carried out in an ambient environment without a protective atmosphere. While measuring the current density-voltage (J–V) curves for DSSCs, a black mask was used and only the effective area of the cell was exposed to light irradiation. The data reported in this paper was confirmed by making each device more than five times.

2.5. Measurement of diffusion coefficient

Diffusion measurements were performed at a thin layer cell, for details see elsewhere [18]. The two electrodes of the cell were made of platinized transparent conducting oxide-coated glass. Platinization has been done by doctor blade and sintering. The electrodes showed a distance of about 60 μm, using sealant. Due to the large variation of the electrode distance, this distance had to be determined for every cell used in diffusion coefficient measurements. Two identical electrodes have been mounted onto each other with sealed by sealant. The polymer electrolytes were filled between two electrodes after sealing using a vacuum pump through tiny filling holes in hot plate. A uniform polymer electrolyte layer was formed at room temperature. The polymer electrolyte was composed of I_2, TBAI, PMII, EC/PC, 3/1 as weight ratio, PAN ($M_w = 86{,}200$, Aldrich Co) or click polymers as a polymer matrix, liquid crystal (ML-0249) (Merck Co) as a plasticizer, and acetonitrile. Impedance spectroscopy was conducted with WEIS500 ZMAN version 2.0 programs. Impedance measurements at thin layer cells were conducted over a frequency range of about 40 kHz to 0.5 MHz.

The finite Warburg impedance does only include the diffusion of the I_3^- ion, because the I^- ion is like a supporting electrolyte and the diffusion coefficient of both species are in nearly the same order of magnitude. The impedance was given by:

$$Z(\omega) = R_D \frac{\tanh\left(\sqrt{i\omega\tau_D}\right)}{\sqrt{i\omega\tau_D}}$$

where R_D has the dimension Ω, the parameter τ_D is associated to the diffusion coefficient and the Nernst-distance of δ to the electrode, where the concentration of the diffusion-limiting species is constant. For thin layer cells this constraint is fulfilled for a distance of $\delta = l/2$ and for τ_D follows:

$$\tau_D = \frac{\delta^2}{D_{I_3^-}} = \frac{(1/2)^2}{D_{I_3^-}} \quad C_{I_3^-}(\delta, t) = \text{const.}$$

yielding the diffusion coefficient of the I_3^- ion. The impedance are shown in Fig. 5 and the diffusion of the I_3^- ion are summarized in Table 2.

3. Results and discussion

Fig. 1 shows the two different click polymerization routes, Cu^I-catalyzed and non-Cu^I-catalyzed methods, between the 2,7-diazido-9,9-dioctylfluorene and 2,7-diethynyl-9,9-dioctylfluorene monomers. We synthesized the click polymers (P1 and P2) using different click reaction methods and compared their effect on the photovoltaic performance of DSSCs using P1 and P2 as polymer electrolyte components. In order to improve the polymer purity and photovoltaic performance, the precipitated polymers were further purified by Soxhlet extraction with methanol and were finally extracted with chloroform to afford highly purified polymers with narrow polydispersity that were completely soluble in various organic solvents such as chloroform, chlorobenzene, THF, toluene, and xylene. Table 1 summarizes the polymerization results, thermal and electro-optical properties of the polymers. The weight average molecular weights (Mw) were 16,110 and 16,120, respectively. The polydispersity of the polymers were 1.92 and 2.15, respectively. The structure and thermal properties of the polymers were identified by ^{1}H-NMR, infrared (IR) spectroscopy, elemental analysis, differential scanning calorimetry (DSC), and thermogravimetric analysis (TGA) thermograms. The appearance of 1,4-disubstituted 1,2,3-triazole peaks from the polymers at approximately 8.39–8.03 ppm in ^{1}H-NMR and acetylenic proton peaks at 2100 cm^{-1} in IR spectroscopy confirmed the Cu^I-catalyzed polymerization reaction. The other peaks were consistent with the proposed chemical structure of the polymers. As shown in Table 1, isothermal pyrolysis showed that the 1,4-disubstituted 1,2,3-triazole units were lost at approximately 340 °C, followed by polymer decomposition at higher temperatures. The higher thermal stability of the polymers prevented the deformation and degradation of the active layer from the heat induced during the DSSC operation.

Table 1
Polymerization results, thermal, and electro-optical properties of P1 and P2.

	P1	P2
Yield (%)	92	91
Mw[a]	16,110	16,120
PDI[a]	1.92	2.15
DSC (T_g)	115	104
TGA[b]	339	362
Abs_{max} (nm)[c]	348	340
PL_{max} (nm)[c]	375,390,511	390,510
E_g (eV)[d]	2.56	2.39
HOMO	5.76	5.67
LUMO	3.19	3.28

[a] Mw and PDI of the polymers were determined by GPC using polystyrene standards.
[b] TGA was measured at temperature of 5% weight loss for the polymers.
[c] Measured in the thin film onto the quartz substrate.
[d] Determined from edge of absorption spectrum.

The UV-visible absorption and PL data of the polymers were measured in both solution and film states. Fig. 2 shows the UV-visible absorption spectra of the polymers in chloroform solution and in thin films coated onto the quartz substrates. The UV-visible absorption spectra of the polymers were similar in the solution and

Table 2
The photovoltaic performances of DSSCs under 1 sun (100 mW cm^{-2}).

Polymer electrolytes	$D_{I_3^-}$ (10×10^{-7} cm^2/s)	J_{SC} (mA cm^{-2})	V_{OC} (V)	FF (%)	PCE (%)	Area (mm^2)
P1	6.82	10.46	0.65	68.0	4.62	21.003
P1: ML-0249 (1:1)	6.25	10.63	0.65	64.5	4.46	21.876
P1: ML-0249 (1:3)	7.46	10.81	0.65	66.9	4.70	21.606
P2	6.25	10.56	0.60	69.6	4.41	20.001
P2: ML-0249 (1:1)	5.08	10.61	0.60	66.1	4.21	21.537
P2: ML-0249 (1:3)	5.40	10.82	0.60	67.3	4.37	21.225
PAN	4.20	9.07	0.60	64.9	3.53	22.639
PAN: ML-0249 (1:1)	4.47	10.27	0.65	66.8	4.46	19.429
PAN: ML-0249 (1:3)	4.84	10.73	0.65	68.5	4.78	19.974

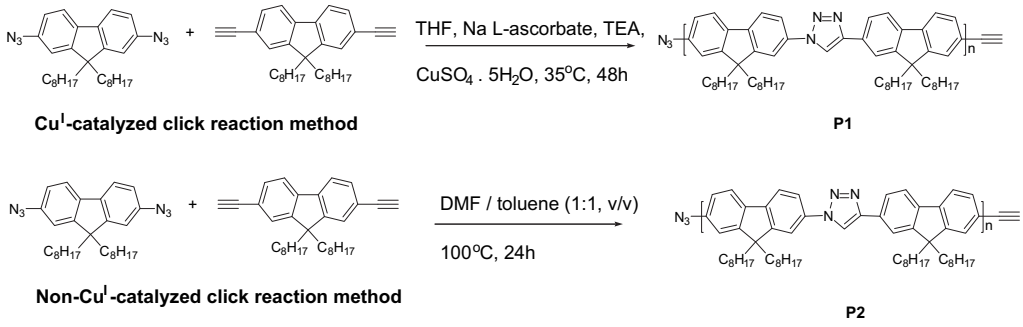

Fig. 1. Synthetic scheme of polymers (P1 and P2).

film states with similar maximum absorption wavelength. This revealed the similar conformation of the polymers in both states with tailing structures in the low energy regions in front of steep, main absorption band edges.

Fig. 3 shows the PL spectra of the polymers in chloroform solution and in the thin film state. The PL spectra of the polymers in chloroform were similar and emitted a blue color between 370 and 395 nm, as shown in Fig. 3a, due to the presence of the fluorene moiety in the polymer chain. Additionally, these blue bands of the polymers had structureless bands centered at the much lower energetic level of approximately 512 nm, because of the introduction of 1,2,3-triazole units with narrow polydispersity in the polymer chain. As shown in Fig. 3b, the PL spectra of the polymers in the film states were slightly different from those of the solution states.

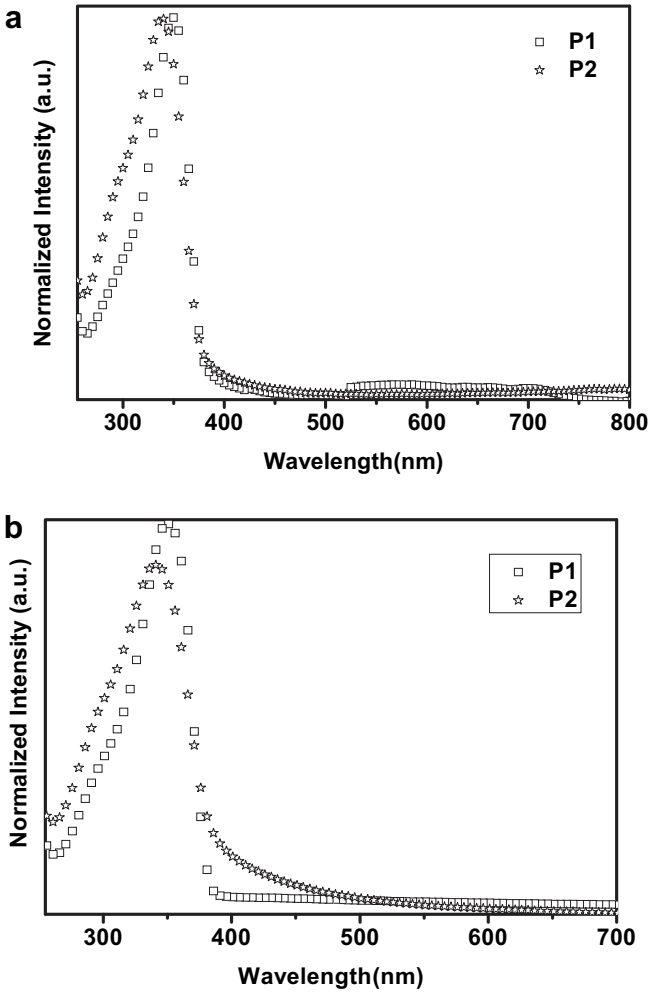

Fig. 2. UV-visible absorption spectra in chloroform (a) and film (b) [concentration 1.5×10^{-4} M] of P1 and P2.

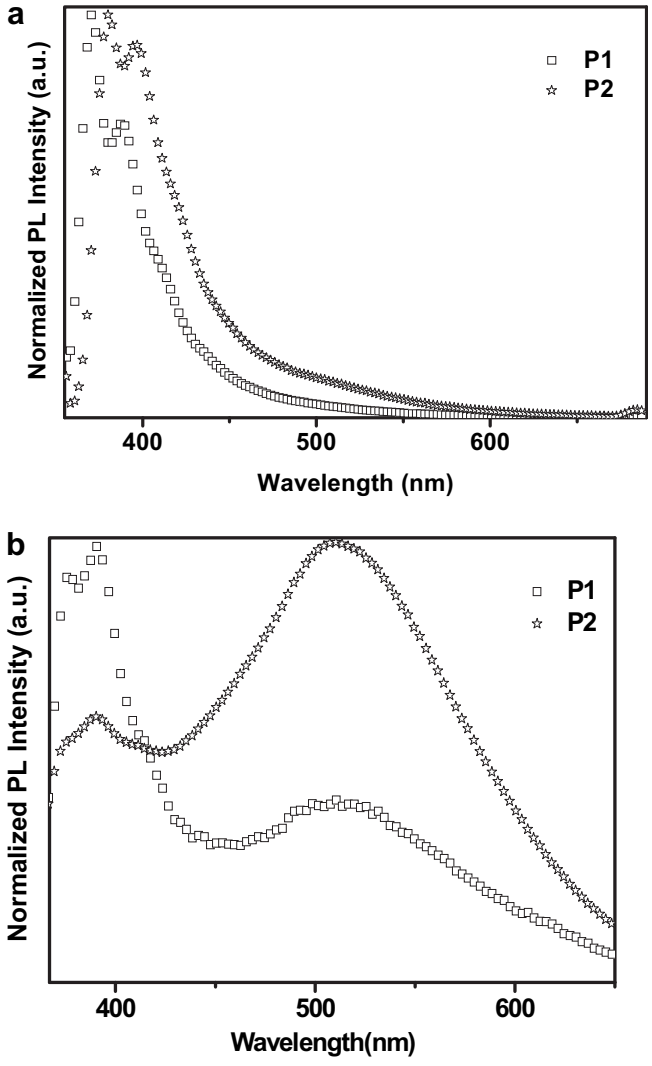

Fig. 3. PL emission in solution (a) and film (b) [concentration 1.5×10^{-4} M] of P1 and P2.

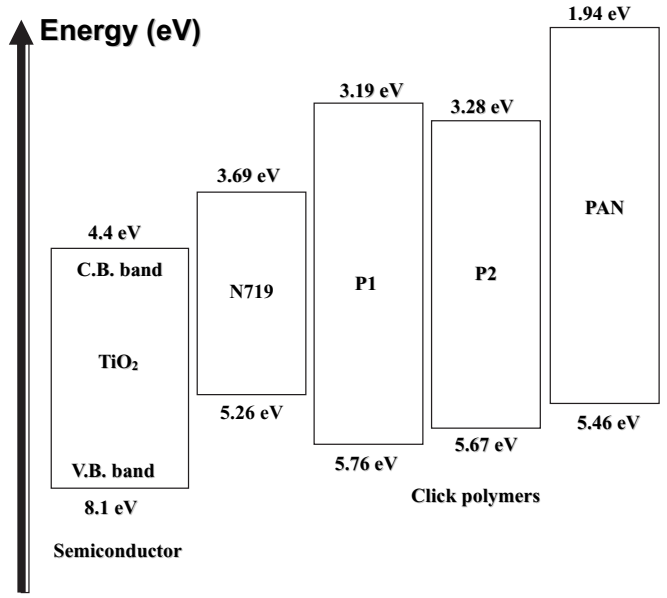

Fig. 4. The energy diagram of polymers and N719 dye.

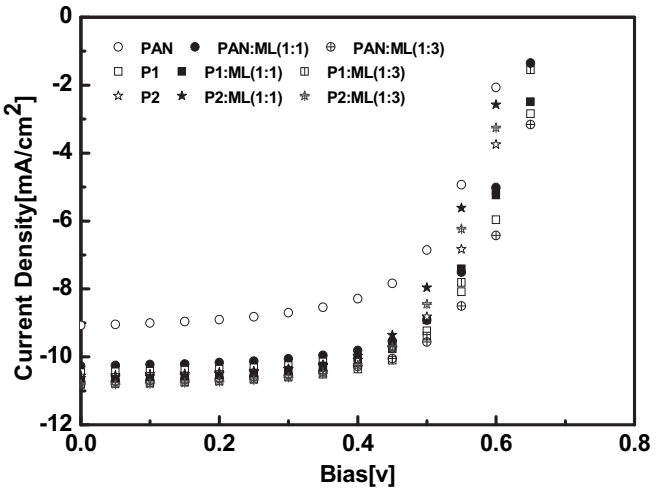

Fig. 5. Photocurrent-voltage characteristics of the DSSCs with polymer electrolyte under AM 1.5 sunlight illumination (100 mW cm^{-2}).

The polymer, P2 had a maximum emission peak at 510 nm with a residual blue band at 390 nm, which were attributed to the non-Cu^{I}-catalyzed click reaction condition and might be due to the mixture of 1,4- and 1,5-substituted 1,2,3-triazole ring [19,20]. The UV-visible absorption and PL spectra of the polymers as thin films are summarized in Table 1.

The highest occupied molecular orbital (HOMO) energies of the polymers with respect to the ferrocene/ferrocenium (4.8 eV) standard were approximately 5.75, 5.67, 5.46, and 5.26 eV for P1, P2, PAN and N719 dye, respectively. From the onsets of the absorption spectra, the band gaps of P1, P2, PAN, and N719 were calculated as 2.56, 2.39, 3.52, and 3.69 eV, respectively. The lowest unoccupied molecular orbital (LUMO) energy levels of the polymers were calculated from the band gaps and HOMO energies and the results are summarized in Table 1 and Fig. 4. It was reported that the HOMO and LUMO energy levels of poly(9,9-dioctylfluorene) measured using an electrochemical method were 5.8 and 2.12 eV, respectively [21]. There is a significant difference in electrochemical behaviour (specially in LUMO) between the reported data and present polymers (P1 and P2), which suggests that the electrochemical properties of the polymers had been altered through the introduction of a 1,4-disubstituted 1,2,3-triazole group between the fluorene units along with the polymer backbone *via* different click reactions. The HOMO levels of polymers were lower than work function of Pt counter electrode and have a proper charge transfer between Pt counter electrode and polymer redox electrolyte [22].

Fig. 5 shows the *J*–*V* curves of the SnO_2:F/TiO_2/N719 dye/polymer electrolyte/Pt device using P1, P2 and PAN as the polymer matrix for the polymer electrolyte at 1 sun condition. The photovoltaic properties of the DSSCs are summarized in Table 2. The DSSCs without ML-0249 (liquid crystal) exhibited a photovoltaic performance with a PCE of 4.62, 4.41, and 3.53% for P1, P2 and PAN, respectively. The PAN-based polymer electrolyte exhibited a lower J_{sc} and PCE than the P1- and P2-based polymer electrolytes. The J_{sc} decrement was attributed to the lowered I_3^- diffusion coefficients, which reduced the supply of I_3^- to the counter electrode and retarded the regeneration of dye [23]. In case of without ML-0249, all click polymers had better photovoltaic performances than PAN-based polymer electrolyte. Among the click polymers, P1 showed the highest photovoltaic performance, with a PCE of 4.62% (V_{oc}: 0.65 V, J_{sc}: 10.46 mA cm^{-2}, FF: 68.0) at 1 sun condition, which allowed the P1-based polymer electrolyte to easily penetrate the dye-adsorbed nc-TiO_2 electrode. These encouraging study results demonstrated that embedding the liquid crystal in the polymer electrolytes improved their photovoltaic performance compared to polymer electrolytes without ML-0249. It is well known that polymer electrolyte is formed by trapping liquid electrolyte in polymer cages. A higher concentration of polymer host produces smaller cage and higher viscosity of the system, ionic movement is limited, which results in the decrease of the ionic conductivity of the polymer electrolyte. Therefore, we blend different weight ratios of liquid crystal with constant weight of polymers. Among the various tested weight ratios of liquid crystals, PAN:ML-0249 (1:3) had the highest photovoltaic performance with a PCE of 4.78% at 1 sun intensity. Because, by using liquid crystal, the viscosity of the electrolyte became low, that provided high diffusion properties of the I_3^- ion. As a result, the performance of DSSC was increased. In case of different click polymers, the Cu^{I}-catalyzed click polymer, P1 with a combination of P1:ML-0249: (1:3)-based DSSCs exhibited a PCE of 4.70% at 1 sun condition (V_{oc}: 0.65 V, J_{sc}: 10.81 mA cm^{-2}, and FF: 66.9). It indicates that with increasing the weight ratio of ML-0249, there was decreased in viscosity of the electrolyte and increased in the J_{sc} and PCE of the DSSCs. These results imply that the weight ratio of ML-0249 in the polymer electrolyte enhanced the diffusion of I_3^-, which causes the increase of J_{sc} and PCE of the DSSCs as shown in Table 2 and Fig. 6. In case of PAN, due to high molecular weight diffusion of I_3^- values were not as like as P1. The recombination of electron and hole may occur through the blocking of hole transfer and it caused slightly decrease of FF of DSSC devices consist of P1 and P2 as shown Table 2. The P2 showed a lower PCE and diffusion of I_3^- coefficient than P1 in both with ML-0249 and without ML-0249 electrolytes based DSSCs devices. It might be due to different polymerization route polymer (P2) and a mixture of 1,4- and 1,5-substituted 1,2,3-triazole ring. There was no significant difference in photovoltaic performance between the P1:ML-0249 (1:3)- and PAN:ML-0249 (1:3)-based based polymer electrolytes, suggesting that the performance of the Cu^{I}-catalyzed click polymer, P1 was similar to that of PAN with ML-0249 in the polymer electrolytes. We are currently investigated new electrolytes for improved DSSC performance.

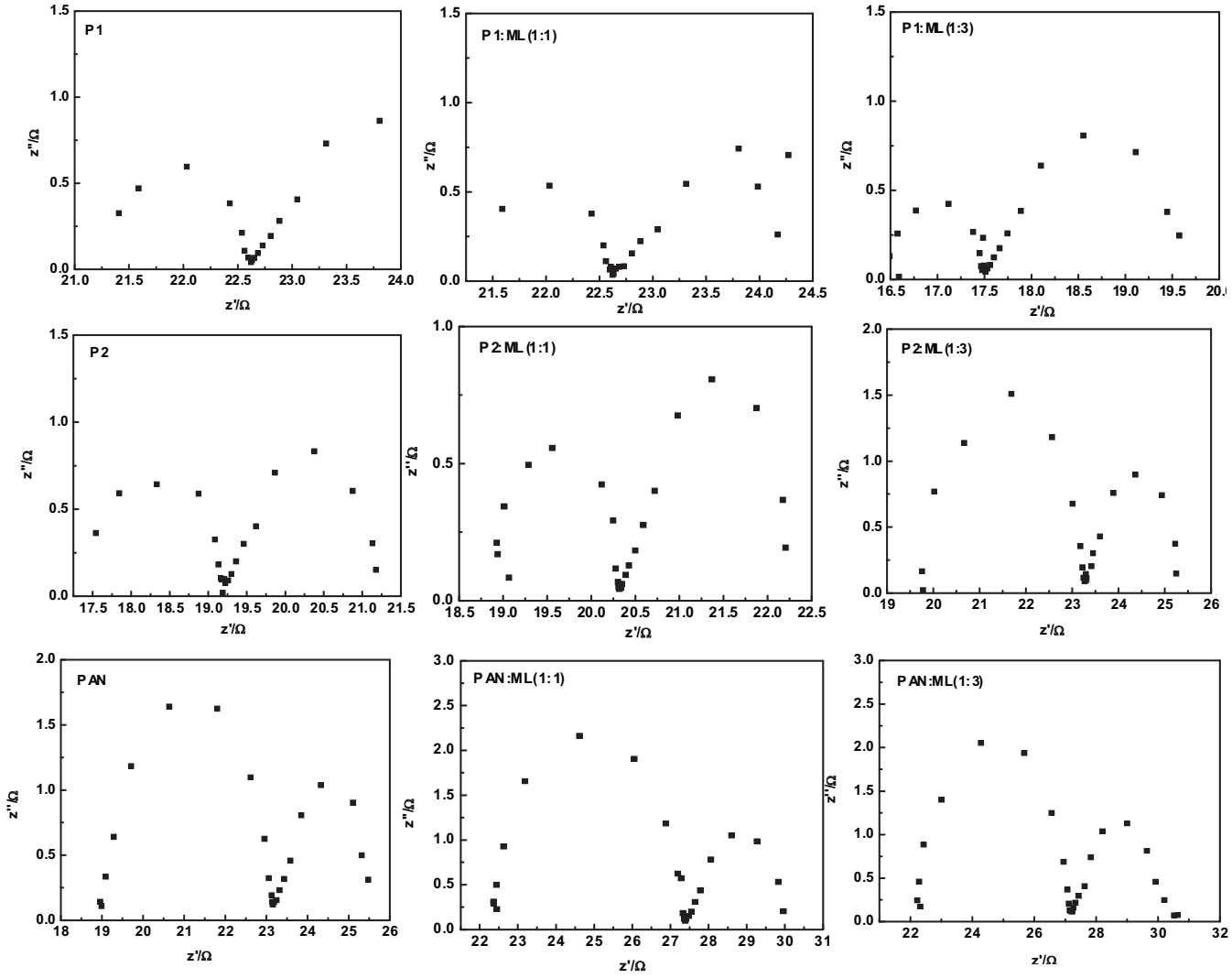

Fig. 6. Nyquist plots for click polymer electrolytes and PAN-based electrolytes with and without liquid crystal ML-0249.

4. Conclusion

We synthesized fluorene-based click polymers using different click reaction polymerization methods and compared their effects on the photovoltaic performance of DSSCs. The embedding of liquid crystals in the polymer electrolytes raised their photovoltaic performance above that of the polymer electrolytes without liquid crystals. The highest PCE of 4.70 and 4.78% at 1 sun were obtained for the DSSCs for P1:ML-0249 (1:3) and PAN:ML-0249 (1:3), respectively, under AM 1.5G illumination with an aperture mask condition. The photovoltaic performance of the Cu^{I}-catalyzed click polymer, P1 was better than that of the other click polymers. Thus, we hope these results will support the application of the Cu^{I}-catalyzed click reaction and click polymer, to facilitate the future use of liquid crystals as electrolyte components in DSSC applications.

Acknowledgments

This work was supported by the Korea Science and Engineering Foundation (KOSEF) grant funded by the Korea government (MOST) (No. M10600000157-06J0000-15710, R11-2008-088-01-003-0). This study was financially supported by Pusan National University in program, Post-Doc. 2008.

References

[1] O'Regan B, Grätzel M. A low-cost, high-efficiency solar cell based on dye-sensitized colloidal TiO2 films. Nature 1991;35:737–40.
[2] Nazeeruddin MK, Kay A, Radices I, Grätzel M. Conversion of light to electricity by cis-X2bis(2,2′-bipyridyl-4,4′-dicarboxylate)ruthenium(II) charge-transfer sensitizers (X = Cl–, Br–, I–, CN–, and SCN–) on nanocrystalline titanium dioxide electrodes. Journal of American Chemical Society 1993;115:6382–90.
[3] Grätzel M. Photoelectrochemical cells. Nature 2001;414:338–44.
[4] Grätzel M. Conversion of sunlight to electric power by nanocrystalline dye-sensitized solar cells. Journal of Photochemical Photobiology A: Chemistry 2004;164:3–14.
[5] Wu JH, Hao SC, Lan Z, Lin JM, Huang ML, Huang YF, et al. A thermoplastic gel electrolyte for stable quasi-solid-state dye-sensitized solar cells. Advanced Functional Materials 2007;17:2645–52.
[6] Wang P, Zakeeruddin SM, Moser JE, Nazeeruddin MK, Sekiguchi T, Grätzel M. A stable quasi-solid-state dye-sensitized solar cell with an amphiphilic ruthenium sensitizer and polymer gel electrolyte. Nature Materials 2003;2:402–7.
[7] Cao F, Oskam G, Searson PC. A solid state, dye sensitized photoelectrochemical cell. Journal of Physical Chemistry 1995;99:17071–3.
[8] Van Steenis DJVC, David ORP, Van Strijdonck GPF, Van Maarseveen JH, Reek JNH. Click-chemistry as an efficient synthetic tool for the preparation of novel conjugated polymers. Chemical Communications 2005;34:4333–5.
[9] Qin A, Jim CKW, Lu W, Lam JWY, Häussler M, Dong Y, et al. Click polymerization: facile synthesis of functional poly(aroyltriazole)s by metal-free, regioselective 1,3-dipolar polycycloaddition. Macromolecules 2007;40:2308–17.
[10] Karim MA, Cho YR, Park JS, Kim SC, Kim HJ, Lee JW, et al. Novel fluorene-based functional 'click polymers' for quasi-solid-state dye-sensitized solar cells. Chemical Communications 2008;16:1929–31.

[11] Kim SC, Song MK, Ryu TI, Lee MJ, Jin SH, Gal YS, et al. Liquid crystals embedded in polymeric electrolytes for quasi-solid state dye-sensitized solar cell applications. Macromolecular Chemistry and Physics 2009;210:1844–50.
[12] Nimura S, Kikuchi O, Ohana T, Yabe A, Kondo S, Kaise M. Effects of additional linkers in biphenyl-4,4′-dinitrene on the low-lying singlet–triplet energy gap and zero-field splitting. Journal of Physical Chemistry A 1997;101:2083–8.
[13] Anuragudom P, Newaz SS, Phanichphant S, Lee TR. Facile Horner–Emmons synthesis of defect-free poly (9,9-dialkylfluorenyl-2,7-vinylene). Macromolecules 2006;39:3494–9.
[14] Liu B, Yu WL, Pei J, Liu SY, Lai YH, Huang W. Design and synthesis of bipyridyl-containing conjugated polymers: effects of polymer rigidity on metal ion sensing. Macromolecules 2001;34:7932–40.
[15] Zhu Y, Huang Y, Meng WD, Li H, Qing FL. Novel perfluorocyclobutyl (PFCB)-containing polymers formed by click chemistry. Polymer 2006;47:6272–9.
[16] Patricia LG, Matyjaszewski K. Click chemistry and ATRP: a beneficial union for the preparation of functional materials. QSAR & Combinatorial Science 2007;26:1116–34.
[17] Koo HJ, Park J, Yoo B, Yoo K, Kim K, Park NG. Size-dependent scattering efficiency in dye-sensitized solar cell. Inorganica Chimica Acta 2008;361:677–83.
[18] Zistler M, Schreiner C, Wachter P, Wasserscheid P, Gerhard D, Gores HJ. Electrochemical characterization of 1-ethyl-3-methylimidazolium thiocyanate and measurement of triiodide diffusion coefficients in blends of two ionic liquids. International Journal of Electrochemical Science 2008;3:236–45.
[19] Qin A, Lam JWY, Jim CKW, Zhang L, Yan J, Häussler M, et al. Hyperbranched polytriazoles: click polymerization, regioisomeric structure, light emission, and fluorescent patterning. Macromolecules 2008;41:3808–22.
[20] Qin A, Lam JWY, Tang L, Jim CKW, Zhao H, Sun J, et al. Polytriazoles with aggregation-induced emission characteristics: synthesis by click polymerization and application as explosive chemosensors. Macromolecules 2009;42:1421–4.
[21] Janietz S, Bradley DDC, Grell M, Giebeler C, Inbasekaran M, Woo EP. Electrochemical determination of the ionization potential and electron affinity of poly(9,9-dioctylfluorene). Applied Physics Letters 1998;73:2453–5.
[22] Lee HJ, Cho YR, Yeo YS, Park SH, Shin WS, Jin SH, et al. Dye-sensitized solar cells with P3HT/Fullerene derivatives. Conference Record of the 2006 IEEE 4th World Conference on Photovoltaic Energy Conversion 2006;1:259–62.
[23] Kim DW, Jeong YB, Kim SH, Lee DY, Song JS. Photovoltaic performance of dye-sensitized solar cell assembled with gel polymer electrolyte. Journal of Power Sources 2005;149:112–5.